Interplay of Isoprenoid and Peptide Substrate Specificity in Protein Farnesyltransferase†

Sarah A. Reigard,‡ Todd J. Zahn,§ Kellie B. Haworth,§ Katherine A. Hicks,|| Carol A. Fierke,|| and Richard A. Gibbs*,‡,§

Department of Medicinal Chemistry and Molecular Pharmacology and Purdue Cancer Center, School of Pharmacy and Pharmaceutical Sciences, Purdue University, West Lafayette, Indiana 47907, Department of Pharmaceutical Sciences, College of Pharmacy and Allied Health Professions, Wayne State University, Detroit, Michigan 48202, and Departments of Chemistry and Biological Chemistry, University of Michigan, Ann Arbor, Michigan 48109

Received April 19, 2005; Revised Manuscript Received June 27, 2005

ABSTRACT: Protein farnesyltransferase (FTase) catalyzes the post-translational modification of many important cellular proteins, and is a potential anticancer drug target. Crystal structures of the FTase ternary complex illustrate an unusual feature of this enzyme, the fact that the isoprenoid substrate farnesyl diphosphate (FPP) forms part of the binding site for the peptide substrate. This implies that changing the structure of FPP could alter the specificity of the FPP−FTase complex for peptide substrates. We have found that this is the case; a newly synthesized FPP analogue, 3-MeBFPP, is a substrate with three peptide cosubstrates, but is not an effective substrate with a fourth peptide (dansyl-GCKVL). Addition of this analogue also inhibits farnesylation of dansyl-GCKVL by FPP. Surprisingly, the differential substrate abilities of these four peptides with FPP−FTase and 3-MeBFPP−FTase complexes do not correlate with their binding affinities for these isoprenoid−enzyme complexes. The possible mechanistic rationales for this observation, along with its potential utility for the study of protein prenylation, are discussed.

Protein prenylation is a critical post-translational modification that is found in ∼1% of mammalian proteins (*1*). Prenylation, either farnesylation or geranylgeranylation, is required for the proper membrane association and activity of many signal transduction proteins. Ras proteins are essential signaling proteins that are farnesylated on the cysteine sulfur of their C-terminal CaaX box, where a is often an aliphatic residue and X is typically either serine or methionine (alanine, glutamine, threonine, and, in certain cases, leucine can also serve as the X residue) (*2*). Oncogenic Ras has been implicated in up to 30% of all human cancers (*3*). The prenylation of Ras is catalyzed by protein farnesyltransferase (FTase).[1] This enzyme transfers a 15-carbon isoprenoid from FPP, farnesyl diphosphate (**1**), to Ras thus allowing for proper membrane association. Due to the fact that Ras must be localized to the plasma membrane to initiate proper signaling, inhibiting this prenylation event has become an area of intense drug development effort for the treatment of cancer. This has led to significant interest in FTase (*2*, *4*), and provided the impetus for the development of FTase inhibitors (FTIs) (*4*, *5*). FTIs have exhibited promising results in certain Phase II and III human clinical trials, and one FTI (Zarnestra from Johnson & Johnson) is under FDA evaluation for the treatment of acute myeloid leukemia (*5*).

The development of FTIs was based on a straightforward paradigm targeting mutant Ras proteins. However, it is not clear that Ras is the sole, or even the most important, target of FTIs (*6*). Database searches indicate that >300 proteins in a typical mammalian cell could be prenylated (*1*). Evidence that other proteins, in particular the small monomeric G protein RhoB (*7*, *8*) and the nuclear kinetochore protein CENP-E (*1*), are key targets of FTIs has been presented. Chemical tools that could selectively modulate protein farnesylation would shed light on the relative roles of various farnesylated proteins in the growth of tumor cells. Here we report the preliminary characterization of the first compound that appears to exhibit this type of desirable selectivity.

FTase catalyzes the transfer of the 15-carbon isoprenoid from FPP to the cysteine sulfur of its protein substrate. Several laboratories have focused on developing a better understanding of the mechanism by which FTase carries out this reaction, and the kinetic scheme is summarized in Figure 1. There was evidence in the early literature that FTase binds its two substrates (FPP and CaaX peptides) in a random order sequential mechanism (*9*). Subsequent studies later refuted that claim (*10*), and now it is widely believed that FTase

† This work was supported in part by NIH Grant CA78819 to R.A.G. and Grant GM40602 to C.A.F. S.A.R. was supported by a Purdue Research Foundation Fellowship. Partial funding was also provided by NIH Training Grant T32 GM08353 (K.A.H.).

* To whom correspondence should be addressed: Department of Medicinal Chemistry and Molecular Pharmacology, 575 Stadium Mall Dr., Purdue University, West Lafayette, IN 47907. Phone: (765) 494-1456. Fax: (765) 494-1414. E-mail: rag@pharmacy.purdue.edu.

‡ Purdue University.

§ Wayne State University.

|| University of Michigan.

[1] Abbreviations: FTase, protein farnesyltransferase; FPP, farnesyl pyrophosphate; FTIs, farnesyltransferase inhibitors; 3-MeBFPP, 3-(3-methyl-2-butenyl)-7,11-dimethyldodeca-2(*Z*),6(*E*),10-triene 1-diphosphate; DIBAL-H, diisobutylaluminum hydride; Fmoc, 9-fluorenylmethyloxycarbonyl; DMF, *N*,*N*-dimethylformamide; HOBt, 1-hydroxybenzotriazole; HBTU, *O*-(benzotriazol-1-yl)-*N*,*N*,*N*′,*N*′-tetramethyluronium hexafluorophosphate; TFA, trifluoroacetic acid.

10.1021/bi050725l CCC: $30.25
Published on Web 07/29/2005

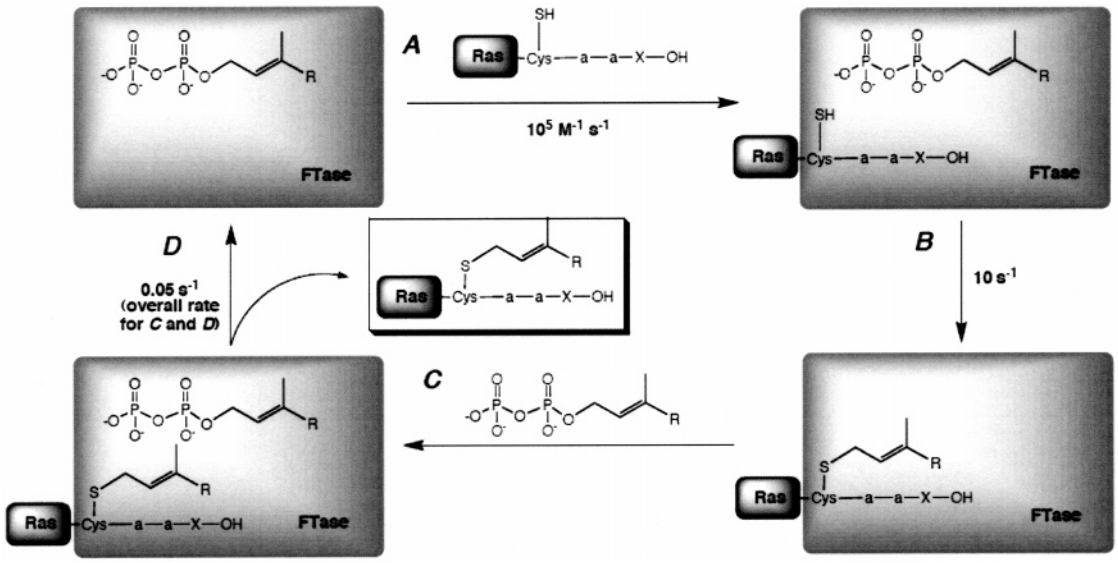

FIGURE 1: General kinetic mechanism for protein farnesyltransferase.

proceeds through a functionally ordered mechanism with FPP binding first with a K_D of ~3 nM (*11*, *12*), followed by binding of the peptide substrate (which also exhibits nanomolar affinity for FTase). A nonreactive complex forms if the peptide substrate binds to FTase before FPP binds (*10*, *11*, *13*). FTase is a metalloenzyme that requires Zn^{2+} bound in the active site to stabilize peptide binding and catalysis (*13*−*15*). The transfer of the farnesyl group to the sulfur of the cysteine is proposed to occur through an S_N2 mechanism involving the nucleophilic attack of the thiolate of the cysteine on C_1 of the isoprenoid whose pyrophosphate could be coordinated with a Mg^{2+} atom (*16*, *17*). Fierke and coworkers determined that the rate constant for the actual chemical transfer of the prenyl moiety to the sulfur is ~10 s^{-1} (*15*) at saturating Mg^{2+} concentrations. After chemistry occurs, FPP-mediated product release is the final and rate-limiting step in the steady-state turnover of this enzyme (*18*). The k_{cat} for the reaction is ~0.06 s^{-1} (*11*).

Recent crystallographic analysis of the FTase−FPP−peptide ternary complex illustrates a striking feature of this enzyme: the isoprenoid moiety of FPP forms part of the binding site for the peptide substrate (*12*, *19*). In fact, Strickland and colleagues reported that in the crystal structure of the ternary complex the peptide contacts both the FTase enzyme and atoms of FPP (*19*). Crystal structures of additional ternary complexes confirm this claim and demonstrate that one FPP isoprenoid unit forms a considerable portion of the peptide binding site with extensive van der Waals interactions (*12*, *20*). In addition, this recent study provided a detailed structural view of the reaction pathway of FTase. The considerable interactions between the FPP and peptide substrates may help explain the specificity differences between FTase and the closely related prenyl transferase, GGTase I (*20*). The discovery of this unusual interaction between the two substrates also leads to the hypothesis that changing the structure of the isoprenoid portion of the FPP substrate could alter the specificity of the FTase−FPP complex for catalyzing farnesylation of peptide substrates.

Previous studies in the Gibbs laboratory have focused on the development of FPP analogues as potential FTIs (*4*, *21*). Chemical methods were developed for the synthesis of multiple FPP analogues modified at the 3 position (*21*−*23*) (such as compounds **2**−**4**) and the 7 position (*24*) as well as geometric isomers and other FPP analogues (*25*). Through these previous studies, nanomolar FTase inhibitors have been characterized in vitro and their effects in cell models have been studied (*21*). In the evaluation of recently synthesized analogues, we obtained surprising results with one compound in particular, 3-MeBFPP (Figure 2, compound **4**). This compound exhibits varying behavior in the presence of distinct peptide cosubstrates. In the presence of the peptide CVLS (**10**), which corresponds to the CaaX box of H-Ras, FTase catalyzes isoprenoid transfer from 3-MeBFPP. This is also the case in the presence of CVIM (**13**), the CaaX box of K-Ras4B, and CKTQ (**12**), which corresponds to the protein CENP-E. Interestingly, when 3-MeBFPP (**4**) is incubated with CKVL (**11**), the CaaX box of RhoB, FTase catalyzes isoprenoid transfer significantly more slowly. Therefore, 3-MeBFPP inhibits farnesylation of CKVL by the natural substrate, FPP. This is the first FPP analogue developed that has the ability to selectively modulate the reactivity of FTase with different peptide substrates. Here we examine the detailed steady-state kinetics of this unusual interaction.

EXPERIMENTAL PROCEDURES

Chemical Synthesis. The 3-isobutenyl FPP analogue (3-MeBFPP) was synthesized from the corresponding farnesol analogue (**9**). Alcohol **9** was prepared in this laboratory as depicted in Scheme 1, and the alcohol was converted to the desired diphosphate 3-MeBFPP (**4**) using the general procedure of Davisson et al. (*26*) as described below.

Procedure for the Preparation of 3-(3-Methyl-2-butenyl)-7,11-dimethyldodeca-2(Z),6(E),10-triene 1-Diphosphate (3-MeBFPP) (4). Vinyl triflate **6** (1.00 g, 2.5 mmol) was subjected to our well-characterized Stille coupling protocol (*22*). Briefly, tributyl(3-methyl-2-butenyl)tin (1.5 equiv, 2.14 g, 5.97 mmol) was dissolved in 3 mL of *N*-methylpyrrolidinone in the presence of catalytic amounts of $Pd(AsPh_3)_2$ (0.398 mmol) and CuO (0.398 mmol) at 100 °C. The vinyl triflate (**6**) was dissolved in 2 mL of *N*-methylpyrrolidinone and added dropwise, and the reaction mixture was stirred

FPP, Analogues, and Inhibitors

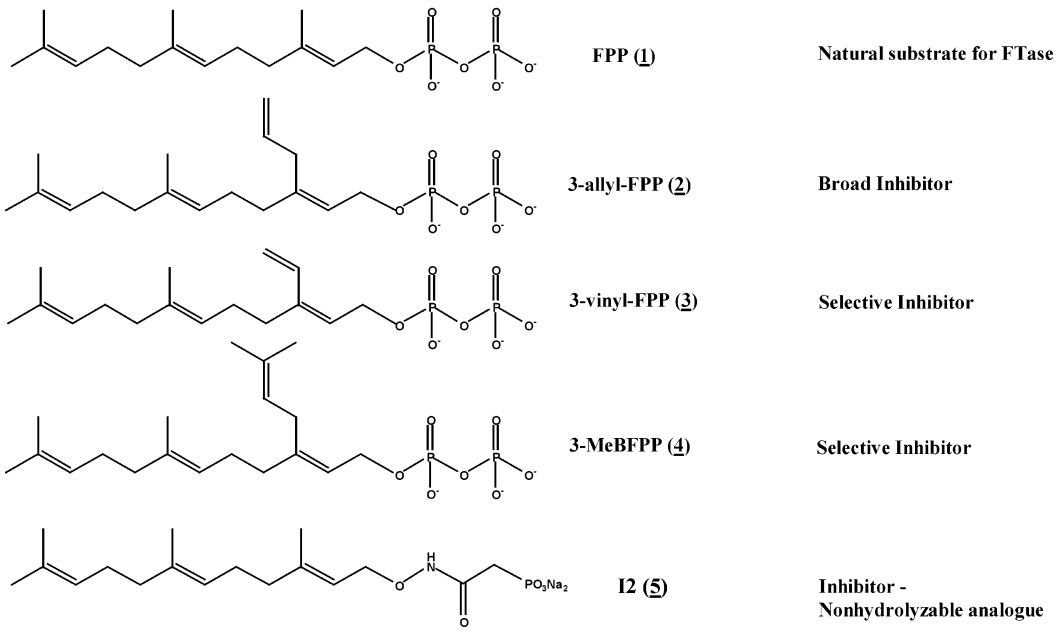

FIGURE 2: Structures of FPP and the analogues discussed in this study.

Scheme 1: Synthesis of 3-MeBFPP (**4**)

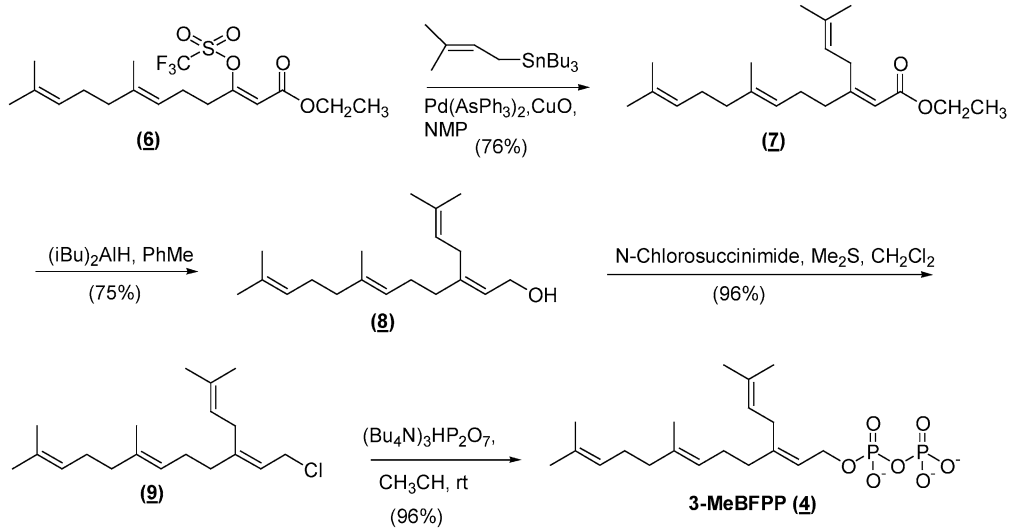

overnight. Following chromatography, the corresponding modified ester (**7**) was obtained (0.795 g, 1.84 mmol, 76% yield). Modified ester **7** (215 mg, 0.676 mmol) was then subjected to DIBAL-H (4 equiv, 2.03 mmol) reduction in toluene to afford alcohol **8** after purification (140 mg, 0.51 mmol, 75% yield). *N*-Chlorosuccinimide (1.5 equiv, 60.0 mg, 0.45 mmol) was dissolved in 3 mL of CH_2Cl_2 (anhydrous under Ar, from Aldrich). The solution was cooled to −30 °C in an acetonitrile/dry ice bath. Methyl sulfide (1.5 equiv, 0.03 mL, 0.45 mmol) was added dropwise, and the resulting milky white mixture was warmed to 0 °C for 5 min and recooled to −30 °C. A solution of 1 equiv of 3-isobutenyl alcohol **8** (80 mg, 0.30 mmol) in 2 mL of dichloromethane was added dropwise to the mixture at −30 °C. The reaction mixture was slowly warmed to 0 °C and stirred for an additional 1 h at that temperature. The resulting clear, colorless solution was stirred at room temperature for 20 min and poured into 10 mL of a cold brine solution. The aqueous layer was extracted with 2 × 15 mL of hexanes, and the combined organic layers were washed with 10 mL of a cold brine solution and dried ($MgSO_4$). After workup, 82 mg (93%) of chloride **9** was obtained as a pale yellow oil that was used directly in the next step. Compound **9** (82 mg, 0.28 mmol) was then treated with tris(tetra-*n*-butylammonium) hydrogen pyrophosphate (556 mg, 1.26 mmol) in 5 mL of acetonitrile for 2 h, and the solvent was removed by rotary evaporation at room temperature. The residue was dissolved in 1−2 mL of ion exchange buffer [1:49 (v/v) 2-propanol/25 mM aqueous NH_4HCO_3 mixture] and was passed through a column containing 100 mL of cation exchange resin (DOWEX AG 50W-X8, NH_4^+ form). The column was eluted with 2 column volumes of ion exchange buffer at a flow rate of ∼1 mL/min. The eluent was dried by lyophilization, and a pale yellow solid was obtained. The crude product was dissolved in 1−3 mL of 25 mM NH_4HCO_3 and purified by cellulose flash column chromatography. Briefly, ap-

proximately 200 mL of cellulose was used, and the diphosphate was loaded onto the column. The column was run using cellulose buffer [1:2:1 (v/v/v) water/2-propanol/acetonitrile mixture and 50 mM NH_4HCO_3] as the eluent. The fractions were collected, pooled, and dried by lyophilization, and 116 mg (96%) of compound **4** (3-MeBFPP) was obtained as a white fluffy solid: ^{1}H NMR (300 MHz, D_2O) δ 1.51 (s, 3H), 1.53 (s, 3H), 1.59 (s, 3H), 1.61 (s, 3H), 1.9−2.10 (m, 8H), 2.80 (br d, 2H), 4.45 (br t, 2H), 4.90−5.10 (m, 3H), 5.40 (br t, 1H); ^{31}P NMR (121 MHz, D_2O) δ −6.23, −9.71; MS negative ESI *m*/*z* 435.

Solid-Phase Peptide Synthesis. The peptide substrates for all experiments were obtained in our lab through solid-phase peptide synthesis. The procedure is briefly described below. Wang resin (200 mg, 0.120 mmol), preloaded with our X amino acid of interest and protected with Fmoc at the primary amine, was subjected to deprotection with 25% piperidine in DMF for 30 min to remove the Fmoc group. Following deprotection and rinsing, coupling of the next Fmoc amino acid (4 equiv, 0.480 mmol) was carried out using 4 equiv (0.480 mmol) of HOBt, HBTU, and diisopropylethylamine in 3 mL of DMF for 3 h. DMF rinsing was done, and the same procedure was repeated to ensure the complete coupling of the amino acid. The dipeptide attached to the resin was then subjected to deprotection with 25% piperidine in DMF for 30 min. After sufficient rinsing, another protected amino acid was coupled using the same protocol described above. Once the desired CaaX sequence was reached, the final coupling involved the addition of dansyl-glycine to the cysteine residue using the same HOBt/HBTU procedure. Following the final coupling, the dansyl-pentapeptide was cleaved from the resin using 90% TFA, 5% triisopropyl silane, and 5% water for 3 h. Following cleavage, peptides were worked up, precipitated with cold ether, and rinsed. All yields were 70−90% and at least 70% pure as determined by HPLC. The HPLC system that was used was an Agilent 1100 HPLC system consisting of an autosampler, a quaternary pump, a UV detector, and a fluorescence detector. The samples were injected onto an analytical C_8 column (Agilent Zorbax Eclipse XDB-C8, 4.6 mm × 150 mm) and eluted with a linear gradient from 70% A and 30% B to 100% B over the course of 30 min (A being 0.025% TFA in water and B being acetonitrile). The peptides were monitored using the fluorescence detector exciting at 340 nm and monitoring emission at 550 nm. All fluorescent peptide substrates (Figure 3) were synthesized as stated above and their identities confirmed by ESI MS. Ds-GCVLS (**10**): MS positive ESI *m*/*z* 711, C_8 reverse-phase HPLC t_R = 1.1 min. Ds-GCKVL (**11**): MS positive ESI *m*/*z* 752, C_8 reverse-phase HPLC t_R = 0.95 min. Ds-GCKTQ (**12**): MS positive ESI *m*/*z* 769, C_8 reverse-phase HPLC t_R = 1.083 min. Ds-GCVIM (**13**): MS positive ESI *m*/*z* 755, C_8 reverse-phase HPLC t_R = 0.98 min.

FTase Fluorescent Assay Procedure. The steady-state kinetic constants for FTase with FPP analogues were determined following a continuous spectrofluorimetric assay originally developed by Pompliano et al. and modified by Poulter and co-workers (*27*, *28*). Utilizing dansylated pentapeptides as cosubstrates, the linear portion of the increase in fluorescence versus time was measured with a Spex FluoroMax2 spectrofluorimeter (excitation wavelength of 340 nm, emission wavelength of 500 nm). The assay components

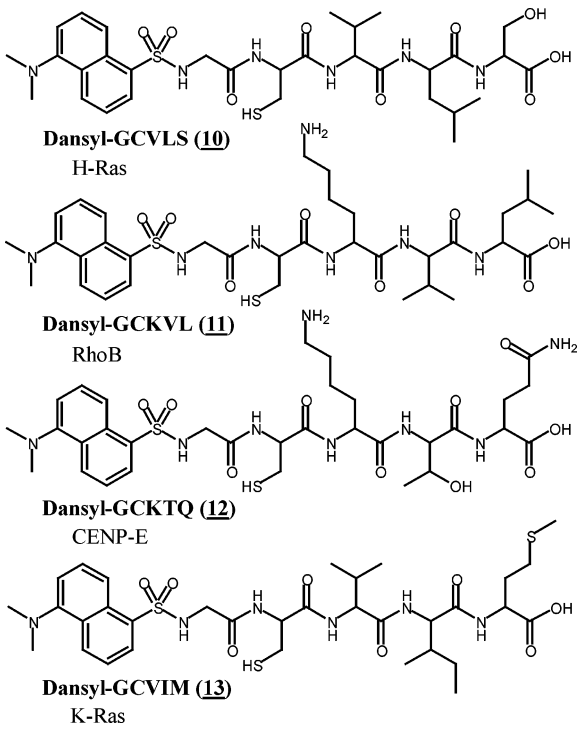

FIGURE 3: Fluorescent peptide substrates.

{444 μL of assay buffer [52 mM Tris-HCl (pH 7.0), 5.8 mM DTT, 12 mM $MgCl_2$, and 12 μM $ZnCl_2$], 6 μL of detergent solution [0.4% *n*-dodecyl β-D-maltoside in 52 mM Tris-HCl (pH 7.0)], and varying volumes of a peptide solution to give the final indicated concentration of peptide [12 μM dansyl-GCVLS, dansyl-GCKVL, dansyl-GCVIM, or dansyl-GCKTQ, as indicated in 20 mM Tris-HCl (pH 7.0) and 10 mM EDTA] with final peptide concentrations between 0.1 and 5 μM} were assembled in a 1.5 mL Eppendorf tube in the order indicated above and were incubated at 30 °C for a period of 5 min. FPP or 3-MeBFPP [~10 mM stock solution in 25 mM ammonium bicarbonate (pH 7.5); final concentration of 1.3 μM] was added to the assay buffer solution. The resulting solution was pipetted into a 0.75 mL quartz cuvette; the reaction was then initiated with addition of recombinant rat FTase [final concentration in the assay of 0.01 μM; expressed in *Escherichia coli* and purified as described previously (*29*)], and fluorescence was detected using a time-based scan at 30 °C for a period of 300 s. The data were fit to the equation $V = (RP)/F_{MAX}$, where V is the velocity of the reaction in micromolar per second, R is the rate of the reaction in counts per second, P is equal to the concentration (micromolar) of FPP (**1**) or 3-MeBFPP (**4**) used in the reaction mixture, and F_{MAX} is the maximum fluorescence intensity obtained as described below.

F_{MAX} Determination. Fluorescence maxima values were obtained in a fashion similar to the FTase assay described above with final concentrations of 6 μM peptide, 5 μM FPP or analogue, and 0.6 μM FTase. The fluorescence value (excitation wavelength of 340 nm, emission wavelength of 500 nm) was obtained after incubation for 60 min at 30 °C. Data are shown in Table 1.

FTase HPLC Assays. Enzyme assay reaction mixtures for HPLC analysis were prepared as follows. The assay components {assay buffer [52 mM Tris-HCl (pH 7.0), 5.8 mM DTT, 12 mM $MgCl_2$, and 12 μM $ZnCl_2$], 25 μM peptide in

Table 1: Determination of Fluorescence Maxima[a]

analogue/peptide	F_{MAX}	analogue/peptide	F_{MAX}
FPP/CVLS	3.16 ± 0.08	FPP/CKTQ	3.57 ± 0.04
3MB/CVLS	4.55 ± 0.03	3MB/CKTQ	3.55 ± 0.17
FPP/CKVL	5.47 ± 0.12	FPP/CVIM	14.17 ± 0.33
3MB/CKVL	2.45 ± 0.05	3MB/CVIM	14.38 ± 0.37

[a] The F_{MAX} values were obtained for each isoprenoid peptide pair as described. The values listed above are actually 1×10^{-6} of the actual values that were obtained (e.g., 3.16 was actually 3 160 000).

assay buffer [250 μM dansyl-GCVLS or dansyl-GCKVL stock solution in 20 mM Tris-HCl (pH 7.0) and 10 mM EDTA]} were assembled in a 1.5 mL Eppendorf tube in the order indicated above and were incubated at 30 °C for a period of 5 min. FPP or 3-MeBFPP [10 mM stock solution in 25 mM ammonium bicarbonate (pH 7.5); final concentration of 5 μM] was added to the assay buffer solution, and the reaction was then initiated with recombinant rat FTase (final FTase concentration of 0.29 μM). The reaction mixture was incubated at 30 °C for the indicated time (5, 30, or 60 min), and a 100 μL aliquot was quenched with an equal volume of acetonitrile. The quenched sample was placed in a vial, which was then loaded into an autosampler. The Agilent 1100 HPLC system consists of an autosampler, a quaternary pump, a UV detector, and a fluorescence detector. The samples were injected onto an analytical C_8 column (Agilent Zorbax Eclipse XDB-C8, 4.6 mm × 150 mm) and eluted with a linear gradient from 70% A and 30% B to 100% B over 30 min (A being 0.025% TFA in water and B being acetonitrile). Retention times for unfarnesylated peptides were between 0.9 and 1.5 min, while the farnesylated peptides had a much higher retention times (14−21 min) due to the addition of the hydrophobic group to the amino acid sequence. The areas of the fluorescent peaks corresponding to the unfarnesylated and farnesylated peptides were determined, and the extent of the reaction was calculated from their ratio.

3-MeBFPP Inhibition of FTase-Catalyzed Farnesylation of Dansyl-GCKVL with FPP. Initial rates at each concentration of 3-MeBFPP were determined using the standard fluorescence assay procedure described above, with fixed concentrations of FPP (1.35 μM) and dansyl-GCKVL (0.7 μM) (Figure 4). The apparent IC_{50} value was estimated by fitting the data to eq 1. However, since 3-MeBFPP is actually a substrate, the apparent inhibition reflects a decreased rate of turnover with 3-MeBFPP compared to FPP. The value of IC_{50} reflects the values of K_M for FPP and 3-MeBFPP and the concentration of FPP, as described by eq 2.

$$v/v_0 = v_{final}/v_0 + [(v_0 - v_f)/v_0]/(1 + [\text{3-MeBFPP}]/IC_{50}) \quad (1)$$

$$IC_{50} = K_M{}^{3-MeBFPP}(1 + [FPP]/K_M{}^{FPP}) \quad (2)$$

Sequential Addition Experiment. A sequential addition experiment was carried out to determine if the binding of the 3-MeBFPP−Ds-GCKVL product to FTase is irreversible. First, FTase was incubated with 3-MeBFPP (1.35 μM) and Ds-GCKVL (0.7 μM) under standard reaction conditions, and the fluorescence was monitored for 600 s. At 600 s, an equal concentration of Ds-CVLS peptide (0.7 μM) was added to the reaction and an immediate and significant increase in fluorescence was observed (Figure 5).

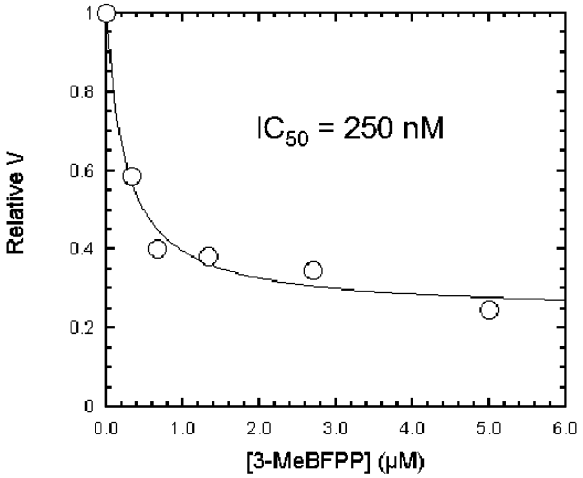

FIGURE 4: Inhibition of CKVL farnesylation by 3-MeBFPP. The relative velocities of the standard reaction of Ds-GCKVL with FPP were obtained at varying concentrations of 3-MeBFPP. From this graph, an IC_{50} of 250 nM was calculated.

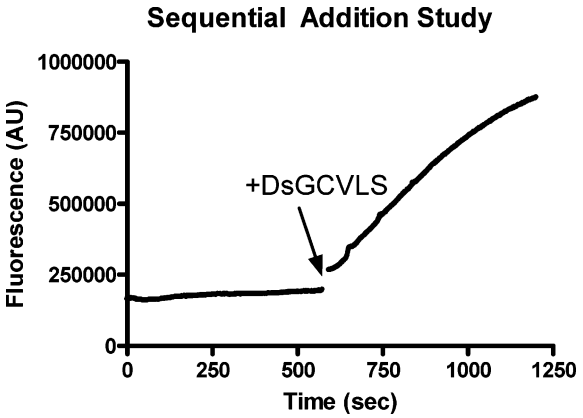

FIGURE 5: Sequential addition study. The fluorescence emission at 500 nm was monitored in a time-dependent manner from 1 to 600 s for a reaction mixture containing 0.7 μM Ds-GCKVL, 1.3 μM 3-MeFPP, and 0.01 μM FTase. At 600 s, 0.7 μM Ds-GCVLS peptide was added, and a significant time-dependent increase in fluorescence was observed due to the transfer of the 3-MeB isoprenoid to Ds-GCVLS.

Determination of the IC_{50} Value for Dansyl-GCKVL Inhibition of FTase-Mediated Prenylation of Dansyl-GCVLS with 3-MeBFPP. Reaction rates at each indicated dansyl-GCKVL concentration were determined using the standard fluorescence assay procedure described above, with fixed concentrations of 3-MeBFPP (1.35 μM) and dansyl-GCVLS (0.7 μM) and varying concentrations of dansyl-CKVL (0−1.3 μM). Each reaction mixture was composed of the FPP analogue and both peptides present in solution, and the reaction was then initiated by the addition of FTase (0.01 μM). The IC_{50} value of 510 nM was estimated from the plot of the relative velocity (V_i/V_o) versus dansyl-GCKVL concentration (Figure 6). Again, this apparent inhibition reflects the slower rates of reaction of dansyl-GCKVL with 3-MeBFPP compared to that with dansyl-GCVLS, and the value of IC_{50} is determined by the K_M values for the two substrates.

Determination of Peptide K_D Values for FTase−Isoprenoid Complexes. The binding of dansylated peptides to the

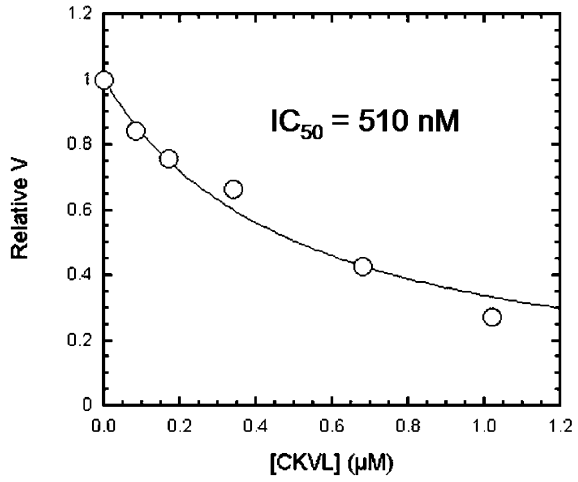

FIGURE 6: CKVL inhibits the prenylation of CVLS with 3-MeBFPP. The velocity for the standard reaction of Ds-GCVLS with 3-MeBFPP at varying concentrations of Ds-GCKVL was monitored. The plot shows that the reaction of Ds-GCVLS with 3-MeBFPP was inhibited by the addition of Ds-GCKVL with an estimated IC_{50} value of 510 nM and an end point or 0.2 relative velocity.

FTase−isoprenoid complex was observed by fluorescence resonance energy transfer, where the tryptophan residues of FTase are excited at 280 nm and the bound dansyl group emits at 496 nm (*13*). The samples were prepared with 50 mM Heppso (pH 7.8), 0.0572 M NaCl, 2 mM TCEP, 20 nM EDTA, and the inactive Y300F mutant of FTase at 40 nM (*30*). The isoprenoid substrate was added [either 80 nM FPP, MeBFPP, or I2, a nonhydrolyzable FPP analogue (Calbiochem)], and the sample was preincubated for 15 min. Then dansylated peptide (Ds-GCVLS, Ds-GCKVL, Ds-GCKTQ, or Ds-GCVIM) was titrated into the solution, and the resulting increase in fluorescence was monitored. These titration experiments were completed within 35 min to minimize the formation of product. [The single-turnover rate constant for farnesylation of GCVLS catalyzed by Y300F FTase under these conditions is 0.0002 s^{-1} (*30*).] The dissociation constant was determined from a fit of a binding isotherm to these data. Alterations in the structure of the peptide and the isoprenoid affect both the peptide affinity and the maximal fluorescence change observed upon binding to FTase.

RESULTS

The Analogue 3-MeBFPP Is a Peptide Selective Substrate for FTase. FTase activity is routinely measured using the fluorescence assay (*28*) described in the Experimental Procedures with a dansylated peptide substrate bearing the CaaX box of H-Ras (dansyl-Gly-Cys-Val-Leu-Ser). In the fluorescence assay with Ds-GCVLS as the peptide substrate, both FPP and 3-MeBFPP were accepted substrates for the enzyme, as shown in Table 2 (with $k_{cat}/K_M^{peptide}$ values of 0.19 and 0.083 μM^{-1} s^{-1}, respectively). This was confirmed by HPLC analysis of the reaction product (data not shown). We then used the alternative peptide substrate dansyl-Gly-Cys-Lys-Val-Leu-OH (Ds-GCKVL), representing the CaaX box of the potential FTI target RhoB. Despite the fact that RhoB possesses a canonical GGTase I CaaX box, it is an effective substrate for both FTase and GGTase I (*8*, *31*). However, this is NOT the case when FPP is replaced in the assay by FPP analogue 3-MeBFPP, as the FTase-catalyzed prenylation is quite slow. HPLC analysis showed only minimal formation (<5%) of the 3-MeB-farnesylated product after 1 h with 25 μM peptide (CKVL) and 5 μM prenyl diphosphate (data not shown). Note this is less product formed than predicted from the steady-state kinetics measured in the next section, perhaps due to product inhibition. The FTase-mediated prenylation of the CaaX box of the K-Ras oncoprotein (Ds-GCVIM) at saturating substrate concentrations is also significantly slower with 3-MeBFPP than FPP, but the turnover number for prenylation of the potential FTI target CENP-E (Ds-GCKTQ) appears to be more efficient with 3-MeBFPP as a substrate.

Kinetic Analysis of FTase Analogue/Peptide Pairs. To investigate the low reactivity of 3-MeBFPP with CKVL compared to those with other peptides in more detail, we measured the peptide concentration dependence of turnover with FPP or the analogue 3-MeBFPP and the four potential peptide substrates, Ds-GCVLS, Ds-GCKVL, Ds-CKTQ, and Ds-CVIM. The peptide concentration was varied because we assumed that (a) the changes in the isoprenoid structure alter the peptide substrate affinity or reactivity and (b) the reactivity with the peptide is key for protein selectivity in vivo. The largest effect of substituting FPP with 3-MeBFPP on the FTase-catalyzed reaction is observed for the peptide Ds-CKVL; substitution of FPP with 3-MeBFPP has deleterious effects on both $K_M^{peptide}$ and k_{cat}, leading to an ~11-fold decrease in the $k_{cat}/K_M^{peptide}$ versus the FPP/Ds-GCKVL pair (Table 2), as determined using the FTase fluorescence assay. Similarly, FPP is a better substrate than 3-MeBFPP with the CKTQ peptide which has a higher $K_M^{peptide}$ and a lower $k_{cat}/K_M^{peptide}$. In contrast, there is at most a 3-fold difference in the steady-state kinetic parameters (k_{cat}, $K_M^{peptide}$, and $k_{cat}/K_M^{peptide}$) between the FPP/Ds-GCVLS and 3-MeBFPP/Ds-GCVLS substrate pairs. The Ds-GCVIM peptide has similar reactivity with both FPP and the analogue; however, the $k_{cat}/K_M^{peptide}$ values for both pairs are lower than that for the FPP/Ds-CVLS pair. The relative reactivities of the eight substrate pairs were confirmed by HPLC analysis (data not shown).

3-MeBFPP Inhibits CKVL Farnesylation. The data given above demonstrate that 3-MeBFPP is an efficient substrate with Ds-GCVLS, but not with Ds-GCKVL. On this basis, we examined the ability of 3-MeBFPP to inhibit farnesylation of Ds-GCKVL by FPP. As expected from the decreased value of $k_{cat}/K_M^{peptide}$, 3-MeBFPP appears to inhibit FPP-mediated farnesylation of Ds-GCKVL with an apparent IC_{50} of ~250 nM (Figure 4). However, the rate of turnover is only decreased a maximum of ~3-fold at high 3-MeBFPP concentrations, as predicted from the decrease in the values of k_{cat} (0.045 s^{-1} for FPP and 0.015 s^{-1} for 3-MeBFPP) and F_{MAX} (Tables 1 and 2). Since 3-MeBFPP is a substrate, the value of IC_{50} should reflect the value of $K_M^{CKVL/3-MeBFPP}$ (see eq 2). Note that in the presence of CVLS $K_m^{3-MeBFPP} = 800$ nM (data not shown). Although 3-MeBFPP appears to function as an inhibitor, this compound is actually serving as a substrate, although with slower kinetics. Thus, $K_{I-apparent}$ cannot be determined from a standard double-reciprocal plot ($1/v$ vs $1/[I]$) at varying peptide and 3-MeBFPP concentrations since activity decreases as the 3-MeBFPP concentration increases but does not approach zero. The double-reciprocal plot would be curved due to this fact and would prove to be difficult to interpret. The K_I measured for inhibition of CKVL

Table 2: Kinetic Data for the Analogue/Peptide Pairs

diphosphate	peptide	k_{cat} (s^{-1})	$K_M^{peptide}$ (μM)	$k_{cat}/K_M^{peptide}$ (s^{-1} μM^{-1})	$K_{d\,(peptide)}$ (μM)
FPP (**1**)	Ds-GCVLS	0.13 ± 0.01	0.7 ± 0.2	0.19 ± 0.04	0.18 ± 0.04
FPP (**1**)	Ds-GCKVL	0.045 ± 0.008	0.7 ± 0.3	0.06 ± 0.02	16 ± 3
FPP (**1**)	Ds-GCKTQ	0.022 ± 0.004	0.5 ± 0.2	0.044 ± 0.011	$>380 \pm 50$
FPP (**1**)	Ds-GCVIM	0.010 ± 0.001	0.16 ± 0.05	0.06 ± 0.02	0.055 ± 0.006
3-MeBFPP (**4**)	Ds-GCVLS	0.058 ± 0.013	0.7 ± 0.4	0.08 ± 0.04	0.074 ± 0.009
3-MeBFPP (**4**)	Ds-GCKVL	0.015 ± 0.006	2.5 ± 1.7	0.006 ± 0.002	1.3 ± 0.2
3-MeBFPP (**4**)	Ds-GCKTQ	0.033 ± 0.004	1.8 ± 0.6	0.018 ± 0.004	$>350 \pm 20$
3-MeBFPP (**4**)	Ds-GCVIM	0.009 ± 0.001	0.14 ± 0.08	0.06 ± 0.04	0.021 ± 0.004
I2	Ds-GCVLS	ND	ND	ND	0.25 ± 0.02
I2	Ds-GCKVL	ND	ND	ND	2.1 ± 0.4
I2	Ds-GCKTQ	ND	ND	ND	0.25 ± 0.02
I2	Ds-GCVIM	ND	ND	ND	0.20 ± 0.02

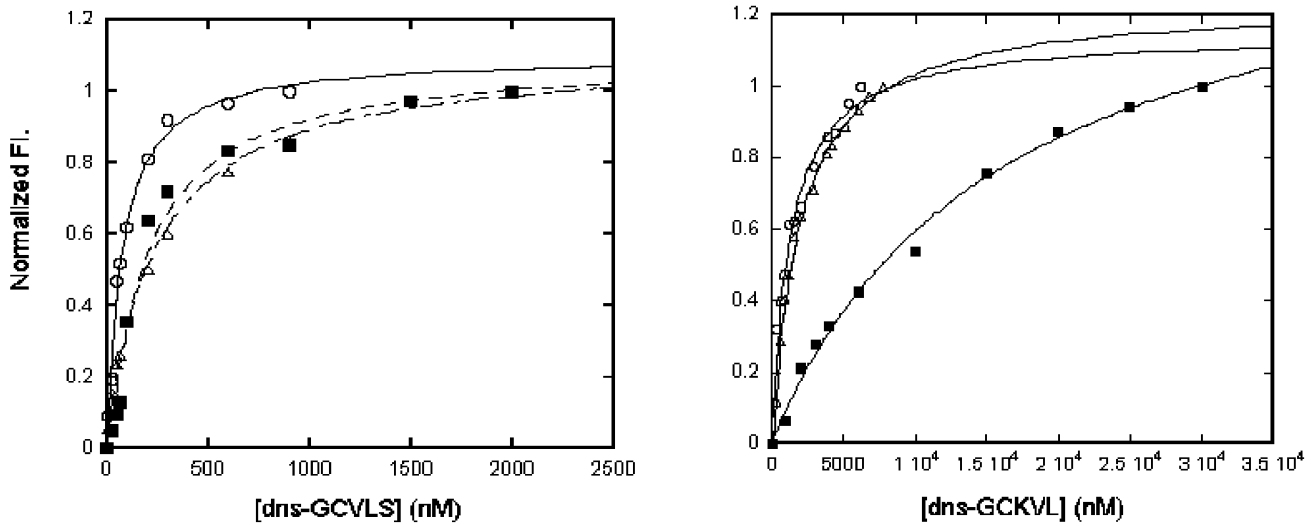

FIGURE 7: Representative peptide K_D plots for FTase−isoprenoid complexes. The K_D plots were obtained at described. The samples were prepared with 50 mM Heppso (pH 7.8), 0.0572 M NaCl, 2 mM TCEP, 20 nM EDTA, and 40 nM Y300F FTase. The isoprenoid substrate was added [80 nM FPP (○), MeBFPP (■), or I2 FPP analogue (△) (Calbiochem)], and the sample was preincubated for 15 min. Then aliquots of the dansylated peptide (Ds-GCVLS or Ds-GCKVL) were added, and the fluorescence was determined. (A) For Ds-GCVLS, $K_d^{FPP} = 0.18 \pm 0.04$ μM, $K_d^{MeBFPP} = 0.074 \pm 0.009$ μM, and $K_d^{I2} = 0.25 \pm 0.02$ μM. (B) For Ds-GCKVL, $K_d^{FPP} = 16 \pm 3$ μM, $K_d^{MeBFPP} = 1.3 \pm 0.2$ μM, and $K_d^{I2} = 2.1 \pm 0.4$ μM.

farnesylation by 3-MeBFPP should equal the K_M value measured from steady-state kinetics (see eq 2).

K_D Determinations for the Analogue/Peptide Pairs. FTase exhibits complex kinetic behavior (*15*, *30*). In particular, peptide association and product dissociation, rather than chemistry, are the rate-limiting steps in $k_{cat}/K_M^{peptide}$ and k_{cat}, respectively, for the FTase-catalyzed farnesylation of H-Ras peptide mimics. Thus, the steady-state kinetic parameters provide little insight into the relative binding affinities and chemical rate constants exhibited by the substrate pairs. To determine whether the altered prenyl diphosphate affects the binding affinities of the four dansylated peptides, the peptide binding affinities for the FTase−FPP and FTase−3-MeBFPP complexes were determined (Table 2 and Figure 7) using the Y300F mutant of FTase in the absence of magnesium to block the reaction of the ternary substrate complex (*30*). For this set of substrates, the measured values of $K_{d(peptide)}$ vary more than 10^4-fold while the values of $k_{cat}/K_M^{peptide}$ vary 30-fold, at most (Table 2). These data demonstrate that there is little or no correlation between $k_{cat}/K_M^{peptide}$ and $K_{d(peptide)}$. However, the peptide binding affinity is altered as the structure of the bound isoprenoid varies with the largest effects observed for substitution of a prenyl diphosphate with the I2 analogue (up to 350-fold). Furthermore, these data illustrate that catalytic reactivity, as measured by $k_{cat}/K_M^{peptide}$, and not substrate affinity is the relevant parameter for the determination of substrate selectivity in vitro and in vivo.

Addition of Ds-GCVLS to a Ds-GCKVL/3-MeBFPP Reaction Leads to Enhanced FTase Turnover. The kinetic complexity of FTase may also have implications for the observed protein selectivity. It is likely that the slow turnover number measured for the reaction of 3-MeBFPP with Ds-GCKVL is due to the slow dissociation of the prenylated peptide product from FTase. The dissociation rate constant is normally enhanced by the binding of additional substrate molecules (*11*, *12*, *18*). We have evaluated the ability of 3-MeBFPP and Ds-GCKVL to react and form a slowly dissociating product as follows. Peptide Ds-GCKVL (0.7 μM) and 3-MeBFPP (1.35 μM) were incubated with 0.01 μM FTase for 10 min, during which time only a minimal increase in fluorescence intensity was observed. Ds-GCVLS was then added to the reaction mixture, and an immediate linear increase in fluorescence intensity and thus presumably the level of product formation was observed (Figure 5), indicating that the 3-MeBFPP−Ds-GCKVL and/or the prenylated product is not bound to FTase in an irreversible manner. This increase in rate is consistent with previously measured rate constants (Table 2). We note that (a) the initial velocity of the second reaction varies with the concentration of Ds-GCVLS and (b) the initial rate of prenylation of Ds-

GCVLS catalyzed by FTase using 3-MeBFPP as the cosubstrate is inhibited significantly by the addition of Ds-GCKVL, with an apparent IC_{50} for Ds-GCKVL of 510 nM. This inhibition is more potent than might be predicted from the steady-state kinetic parameters which suggest that the IC_{50} should be comparable to the $K_M^{peptide}$ (2.5 μM).

DISCUSSION

Our initial hypothesis and motivation for these studies were based on the crystal structures of the FTase−FPP−peptide ternary complex, which illustrate that the isoprenoid moiety of FPP forms part of the binding site for the peptide substrate (*12*). This suggested that modification of the farnesyl moiety could thus lead to looser or tighter binding of the peptide or protein substrates to the enzyme. Here we have demonstrated that it is possible for a diphosphate analogue to alter the peptide substrate selectivity of FTase. Several FPP analogues have also been evaluated for the type of selective substrate behavior exhibited by 3-MeBFPP.[2] Our data suggest that modifying the isoprenoid ligand can alter the specificity of the enzyme for its peptide substrate. Other researchers have shown that FTase has different specificity for peptides substrates in the presence of FPP and GGPP (*32, 33*). Also, it has been shown that FTase can utilize various isoprenoids, FPP, GGPP, and GPP, as prenyl donors in the presence of various peptide substrates (*10*). However, this report is the first to show this specificity with modified FPP analogues.

The mechanism by which this altered substrate specificity occurs has yet to be determined. Due to the complexity of the kinetic mechanism for FTase and the difficulty in measuring kinetic constants at each point in the reaction pathway, the exact altered step is unclear. The kinetic parameter $k_{cat}/K_M^{peptide}$ measures the steps in the reaction starting from the FTase−FPP complex through the first, irreversible step which is the farnesylation step (Figure 1A,B) (Pais and C. A. Fierke, unpublished data); therefore, there are three general steps that could be affected by the structure of the isoprenoid substrate. First, FPP analogue 3-MeBFPP could alter the ability of the various peptide substrates to bind to the diphosphate−enzyme complex. This was the initial thought when the data were collected and the phenomenon was observed (*12*). However, the measured affinities of peptides for the prenyl diphosphate−FTase complex do not correlate with the kinetic data indicating that the altered specificity is not caused by changes in peptide affinity. For example, the decreased reactivity of the Ds-GCKVL peptide with 3-MeBFPP could have been caused by a decrease in peptide affinity. However, this was not observed as the $K_{d(peptide)}$ values for Ds-GCKVL are 1.3 and 16 μM for 3-MeBFPP−FTase and FPP−FTase complexes, respectively. Alternatively, the structure of the isoprenoid diphosphate could alter the apparent association rate constant for the peptide, rather than the binding affinity, thereby altering the value of $k_{cat}/K_M^{peptide}$.

A second possible explanation is that the altered structure of the prenyl diphosphate analogue (Figure 1) decreases the chemical rate constant and this causes a decrease in the value of $k_{cat}/K_M^{peptide}$. Although the farnesylation rate constant is not rate-limiting for either k_{cat} or $k_{cat}/K_M^{peptide}$ for efficient substrates (*18*), it is possible that this step is decreased so significantly for the FTase−3-MeBFPP−Ds-GCKVL complex that it becomes rate-limiting. There would have to be a drastic change in the rate of chemistry, which usually proceeds at $\sim$10 s^{-1}, were it to be slower than the rate constant of substrate dissociation. The correct positioning of C_1 of the prenyl diphosphate relative to the thiolate nucleophile likely has a large effect on the reaction rate constant. Crystal structures of the FTase−FPP−peptide ternary complex all reflect an inactive FPP binding mode where the two reacting atoms, C_1 of FPP and the cysteine thiolate, are more than 7 Å apart, presumably due to the fact that the complexes are formed with components that are catalytically inactive (*12*). The recent crystal structure of the FTase−product complex suggests that, in the catalytically competent ternary complex, the conformation of the FPP molecule is altered where the first and second prenyl units are rotated so that C_1 of FPP is close to the zinc-bound sulfur (*12*). Models of the active ternary complex have been proposed (*12*, *30*). The structure of the isoprenoid substrate could significantly affect the rate constant for rotation of the prenyl units of FPP for formation of the reactive complex and/or the equilibrium between the inactive and active prenyl diphosphate binding modes. To date, neither of these values has been determined for any of the FTase substrates. The kinetics and thermodynamics of this step could modulate the value of $k_{cat}/K_M^{peptide}$ and therefore be responsible for substrate selectivity in FTase.

Finally, the rate constant for product release may be sensitive to the structure of the prenyl diphosphate substrate (Figure 1C,D). Although this step is unlikely to significantly affect the value of the steady-state kinetic parameter $k_{cat}/K_M^{peptide}$, which is proposed to govern protein selectivity, previous studies have shown that release of the farnesylated peptide product is the rate-limiting step in the kinetic mechanism of FTase (*18*). Furthermore, this step is accelerated by binding an additional FPP molecule to the enzyme−product complex (Figure 1C) (*18*). After transfer of the isoprenoid to the sulfur of the cysteine to form the farnesylated product, the isoprenoid is flipped out of the active site binding pocket to interact with an additional isoprenoid binding groove (*12*). This allows for binding of the next molecule of FPP and subsequent release of the product (*12*). There are several possible ways in which the isoprenoid structure can alter this step in the reaction pathway. The 3-MeB-farnesylated product may bind more tightly to the enzyme than its farnesylated counterpart and, hence, dissociate more slowly. Alternatively, the conformational changes needed to flip the isoprenoid out to the exit groove may be less favorable, or the ability of an additional molecule of 3-MeBFPP to bind to the active site to increase the rate of product dissociation may be significantly weaker or slower. In particular, the latter mode of selectivity opens up the possibility of unusual variations in turnover rate with varying isoprenoid diphosphate concentrations. The complexity of the enzyme mechanism and the many steps that occur in this reaction pathway make it very difficult to

[2] VinylFPP also is an effective substrate with Ds-GCVLS (uncorrected V_{max}/K_m = 14 000 cps s^{-1} μM^{-1}; K_m = 0.5 ± 0.2 μM) but not with Ds-GCKVL (uncorrected V_{max}/K_m = 940 cps s^{-1} μM^{-1}; K_m = 1.1 ± 0.3 μM). However, in this case, we were not able to determine an IC_{50} for inhibition of FPP-mediated farnesylation of Ds-GCKVL by 3-vinylFPP. Nonetheless, it is possible that the inability of 3-vFPP to prenylate certain proteins may be responsible for the cellular effects elicited by 3-vFOH, a prodrug for 3-vFPP (*21*).

explain the steady-state rate data presented herein. However, the data clearly illustrate the ability of isoprenoid analogues to alter the peptide substrate selectivity of FTase.

The biochemical results described above imply that certain isoprenoid analogues may be able to alter FTase selectivity for its protein substrates in cells. In combination with our finding (*21*) that the alcohol precursors, or certain FPP analogues, can serve to incorporate the isoprenoid into CaaX proteins in cells, and the natural diversity of protein CaaX sequences (*1*), this implies that 3-(3-methyl-2-butenyl)-farnesol could block the farnesylation of certain proteins, such as RhoB (with a CKVL CaaX box) in cells, while allowing for the prenylation of other proteins, such as H-Ras, K-Ras, and CENP-E. A selective inhibitor of the farnesylation of a protein such as RhoB in cells would be a precise chemical tool, in contrast to farnesyltransferase inhibitors (FTIs), which potentially block the modification of all potential farnesylation substrates in a cell. FTIs exhibit anticancer effects in many tumor cells other than Ras-positive ones (*3*). It is likely that the anticancer effects of FTIs are due to the inhibition of the farnesylation of several other proteins, including RhoB (*8*) and CENP-E (*1*). The determination of the identity of these "protein X" targets (*3*) is crucial for the rational use of FTIs in clinical settings.

Alternatively, it may be possible to design or discover FPP analogues that allow for the selective modification of only a single CaaX box protein in a cell. The modification of a single protein with an unnatural isoprenoid would be a valuable tool, complementary to the semisynthetic approaches of Waldmann and co-workers (*34*, *35*), allowing for the manipulation of prenylation in cells. In this case, it may be necessary to introduce via mutagenesis an unnatural CaaX box with unusual selectivity properties into the protein of interest. Such a strategy would be reminiscent of the "bump-hole" approach. Several groups have demonstrated that enzyme (*36*) and receptor (*37*) selectivity can be altered in a selective, rational manner using a combination of site-directed mutagenesis and analogue synthesis. The results presented here suggest that this approach could be used to rationally alter the substrate selectivity of FTase, although in this case the engineering could be done without altering the enzyme itself.

For experiments such as those described above, it would be valuable to understand the rules that cover the interplay of substrate selectivity in FTase. This study was a preliminary attempt to interrogate these rules in a reductive manner via steady-state kinetic investigations. At the current time, a screening approach to elucidating FTase substrate selectivity patterns may be more fruitful. This study has provided both the first example of a unique type of enzyme substrate interplay and insight into the mechanism of this process.

ACKNOWLEDGMENT

We thank Dr. Diwan S. Rawat (Purdue University) for assistance with the synthesis of 3-MeBFPP.

REFERENCES

1. Ashar, H. R., James, L., Gray, K., Carr, D., Black, S., Armstrong, L., Bishop, W. R., and Kirschmeier, P. (2000) Farnesyl transferase inhibitors block the farnesylation of CENP-E and CENP-F and alter the association of CENP-E with the microtubules, *J. Biol. Chem. 275*, 30451−7.
2. Harris, C. M., and Poulter, C. D. (2000) Recent studies of the mechanism of protein prenylation, *Nat. Prod. Rep. 17*, 137−44.
3. Cox, A. D., and Der, C. J. (1997) Farnesyltransferase inhibitors and cancer treatment: Targeting simply Ras? *Biochim. Biophys. Acta 1333*, F51−71.
4. Gibbs, R. A., Zahn, T. J., and Sebolt-Leopold, J. S. (2001) Non-peptidic prenyltransferase inhibitors: Diverse structural classes and surprising anti-cancer mechanisms, *Curr. Med. Chem. 8*, 1437−65.
5. Brunner, T. B., Hahn, S. M., Gupta, A. K., Muschel, R. J., McKenna, W. G., and Bernhard, E. J. (2003) Farnesyltransferase inhibitors: An overview of the results of preclinical and clinical investigations, *Cancer Res. 63*, 5656−68.
6. Sebti, S. M., and Der, C. J. (2003) Opinion: Searching for the elusive targets of farnesyltransferase inhibitors, *Nat. Rev. Cancer 3*, 945−51.
7. Liu, X. H., and Prestwich, G. D. (2002) Didehydrogeranylgeranyl (ΔΔGG): A fluorescent probe for protein prenylation, *J. Am. Chem. Soc. 124*, 20−1.
8. Prendergast, G. C. (2000) Farnesyltransferase inhibitors: Anti-neoplastic mechanism and clinical prospects, *Curr. Opin. Cell Biol. 12*, 166−73.
9. Pompliano, D. L., Rands, E., Schaber, M. D., Mosser, S. D., Anthony, N. J., and Gibbs, J. B. (1992) Steady-state kinetic mechanism of Ras farnesyl:protein transferase, *Biochemistry 31*, 3800−7.
10. Pompliano, D. L., Schaber, M. D., Mosser, S. D., Omer, C. A., Shafer, J. A., and Gibbs, J. B. (1993) Isoprenoid diphosphate utilization by recombinant human farnesyl:protein transferase: Interactive binding between substrates and a preferred kinetic pathway, *Biochemistry 32*, 8341−7.
11. Furfine, E. S., Leban, J. J., Landavazo, A., Moomaw, J. F., and Casey, P. J. (1995) Protein farnesyltransferase: Kinetics of farnesyl pyrophosphate binding and product release, *Biochemistry 34*, 6857−62.
12. Long, S. B., Casey, P. J., and Beese, L. S. (2002) Reaction path of protein farnesyltransferase at atomic resolution, *Nature 419*, 645−50.
13. Hightower, K. E., Huang, C. C., Casey, P. J., and Fierke, C. A. (1998) H-Ras peptide and protein substrates bind protein farnesyltransferase as an ionized thiolate, *Biochemistry 37*, 15555−62.
14. Chen, W. J., Moomaw, J. F., Overton, L., Kost, T. A., and Casey, P. J. (1993) High level expression of mammalian protein farnesyltransferase in a baculovirus system. The purified protein contains zinc, *J. Biol. Chem. 268*, 9675−80.
15. Huang, C. C., Casey, P. J., and Fierke, C. A. (1997) Evidence for a catalytic role of zinc in protein farnesyltransferase. Spectroscopy of Co^{2+}-farnesyltransferase indicates metal coordination of the substrate thiolate, *J. Biol. Chem. 272*, 20−3.
16. Mu, Y. Q., Omer, C. A., and Gibbs, R. A. (1996) On the stereochemical course of human protein-farnesyl transferase, *J. Am. Chem. Soc. 118*, 1817−23.
17. Huang, C., Hightower, K. E., and Fierke, C. A. (2000) Mechanistic studies of rat protein farnesyltransferase indicate an associative transition state, *Biochemistry 39*, 2593−602.
18. Tschantz, W. R., Furfine, E. S., and Casey, P. J. (1997) Substrate binding is required for release of product from mammalian protein farnesyltransferase, *J. Biol. Chem. 272*, 9989−93.
19. Strickland, C. L., Windsor, W. T., Syto, R., Wang, L., Bond, R., Wu, Z., Schwartz, J., Le, H. V., Beese, L. S., and Weber, P. C. (1998) Crystal structure of farnesyl protein transferase complexed with a CaaX peptide and farnesyl diphosphate analogue, *Biochemistry 37*, 16601−11.
20. Reid, T. S., Terry, K. L., Casey, P. J., and Beese, L. S. (2004) Crystallographic analysis of CaaX prenyltransferases complexed with substrates defines rules of protein substrate selectivity, *J. Mol. Biol. 343*, 417−33.
21. Gibbs, B. S., Zahn, T. J., Mu, Y., Sebolt-Leopold, J. S., and Gibbs, R. A. (1999) Novel farnesol and geranylgeraniol analogues: A potential new class of anticancer agents directed against protein prenylation, *J. Med. Chem. 42*, 3800−8.
22. Gibbs, R. A., Krishnan, U., Dolence, J. M., and Poulter, C. D. (1995) A Stereoselective Palladium Copper-Catalyzed Route to Isoprenoids: Synthesis and Biological Evaluation of 13-Methylidenefarnesyl Diphosphate, *J. Org. Chem. 60*, 7821−9.
23. Zahn, T. J., Weinbaum, C., and Gibbs, R. A. (2000) Grignard-mediated synthesis and preliminary biological evaluation of novel

3-substituted farnesyl diphosphate analogues, *Bioorg. Med. Chem. Lett. 10*, 1763−6.
24. Rawat, D. S., and Gibbs, R. A. (2002) Synthesis of 7-substituted farnesyl diphosphate analogues, *Org. Lett. 4*, 3027−30.
25. Shao, Y., Eummer, J. T., and Gibbs, R. A. (1999) Stereospecific synthesis and biological evaluation of farnesyl diphosphate isomers, *Org. Lett. 1*, 627−30.
26. Davisson, V. J., Woodside, A. B., Neal, T. R., Stremler, K. E., Muehlbacher, M., and Poulter, C. D. (1986) Phosphorylation of Isoprenoid Alcohols, *J. Org. Chem. 51*, 4768−79.
27. Pompliano, D. L., Gomez, R. P., and Anthony, N. J. (1992) Intramolecular Fluorescence Enhancement: A Continuous Assay of Ras Farnesyl−Protein Transferase, *J. Am. Chem. Soc. 114*, 7945−6.
28. Cassidy, P. B., Dolence, J. M., and Poulter, C. D. (1995) Continuous fluorescence assay for protein prenyltransferases, *Methods Enzymol. 250*, 30−43.
29. Zimmerman, K. K., Scholten, J. D., Huang, C. C., Fierke, C. A., and Hupe, D. J. (1998) High-Level Expression of Rat Farnesyl: Protein Transferase in *Escherichia coli* as a Translationally Coupled Heterodimer, *Protein Expression Purif. 14*, 395−402.
30. Pickett, J. S., Bowers, K. E., Hartman, H. L., Fu, H. W., Embry, A. C., Casey, P. J., and Fierke, C. A. (2003) Kinetic studies of protein farnesyltransferase mutants establish active substrate conformation, *Biochemistry 42*, 9741−8.
31. Lebowitz, P. F., Casey, P. J., Prendergast, G. C., and Thissen, J. A. (1997) Farnesyltransferase inhibitors alter the prenylation and growth-stimulating function of RhoB, *J. Biol. Chem. 272*, 15591−4.
32. Moores, S. L., Schaber, M. D., Mosser, S. D., Rands, E., O'Hara, M. B., Garsky, V. M., Marshall, M. S., Pompliano, D. L., and Gibbs, J. B. (1991) Sequence dependence of protein isoprenylation, *J. Biol. Chem. 266*, 14603−10.
33. Goldstein, J. L., Brown, M. S., Stradley, S. J., Reiss, Y., and Gierasch, L. M. (1991) Nonfarnesylated tetrapeptide inhibitors of protein farnesyltransferase, *J. Biol. Chem. 266*, 15575−8.
34. Kuhn, K., Owen, D. J., Bader, B., Wittinghofer, A., Kuhlmann, J., and Waldmann, H. (2001) Synthesis of Functional *Ras* Lipoproteins and Fluorescent Derivatives, *J. Am. Chem. Soc. 123*, 1023−35.
35. Watzke, A., Brunsveld, L., Durek, T., Alexandrov, K., Rak, A., Goody, R. S., and Waldmann, H. (2005) Chemical biology of protein lipidation: Semi-synthesis and structure elucidation of prenylated RabGTPases, *Org. Biomol. Chem. 3*, 1157−64.
36. Bishop, A. C., Buzko, O., and Shokat, K. M. (2001) Magic Bullets for Protein Kinases, *Trends Cell Biol. 11*, 167−72.
37. Tedesco, R., Thomas, J. A., Katzenellenbogen, B. S., and Katzenellenbogen, J. A. (2001) The estrogen receptor: A structure-based approach to the design of new specific hormone-receptor combinations, *Chem. Biol. 8*, 277−87.

BI050725L